JGR Biogeosciences

RESEARCH ARTICLE
10.1029/2019JG005238

Special Section:
Carbon Cycling in Tidal Wetlands and Estuaries of the Contiguous United States

The Effect of Fertilization on Biomass and Metabolism in North Carolina Salt Marshes: Modulated by Location-Specific Factors

K. M. Czapla[1], I. C. Anderson[1], and C. A. Currin[2]

[1]Virginia Institute of Marine Science, William & Mary, Gloucester Point, VA, USA, [2]NOAA Beaufort Laboratory, Beaufort, NC, USA

This article is a companion to Czapla et al. (2020) https://doi.org/10.1029/2019JG005509.

Key Points:
- Chamber measurements of marsh net ecosystem exchange must take into account inundation effects to avoid overestimation of CO_2 fluxes
- The response of salt marshes to fertilization is location specific and negatively correlated with pore water sulfide

Supporting Information:
- Supporting Information S1

Correspondence to:
K. M. Czapla,
kmczapla@vims.edu

Citation:
Czapla, K. M., Anderson, I. C., & Currin, C. A. (2020). The effect of fertilization on biomass and metabolism in North Carolina salt marshes: Modulated by location-specific factors. *Journal of Geophysical Research: Biogeosciences*, *125*, e2019JG005238. https://doi.org/10.1029/2019JG005238

Received 3 MAY 2019
Accepted 28 AUG 2020
Accepted article online 9 SEP 2020

Abstract The resilience of salt marshes to sea level rise depends on vertical accretion through belowground biomass production and sediment deposition to maintain elevation above sea level. Increased nitrogen (N) availability from anthropogenic sources may stimulate aboveground biomass production and sediment deposition and, thus, accretion; however, increased N may also negatively impact marsh accretion by decreasing belowground biomass and increasing net CO_2 emissions. A study was conducted in *Spartina alterniflora*-dominated salt marshes in North Carolina, USA, to determine how responses to fertilization vary across locations with different physical and chemical characteristics. Pore water residence time, inundation time, and proximity to tidal creeks drove spatial differences in pore water sulfide, ammonium, and dissolved carbon concentrations. Although annual respiration and gross primary production were greater at the creek edge than interior marsh sites, net ecosystem CO_2 exchange (NEE) was nearly balanced at all the sites. Fertilization decreased belowground biomass in the interior sites but not on the creek edge. Aboveground biomass, respiration, gross primary production, and net CO_2 emissions increased in response to fertilization, but responses were diminished in interior marsh locations with high pore water sulfide. Hourly NEE measured by chambers were similar to hourly NEE observed by a nearby eddy covariance tower, but correcting for inundation depth relative to plant height was critical for accurate extrapolation to annual fluxes. The impact of fertilization on biomass and NEE, and thus marsh resilience, varied across marsh locations depending upon location-specific pore water sulfide concentrations.

Plain Language Summary Salt marshes provide valuable services, such as protecting the coast from storms, removing excess nutrient pollution from water, and long-term burial of carbon. Because sea level is currently rising, salt marshes need to build up elevation at the same rate as sea level rise to survive. Human-produced nitrogen pollution is rising in salt marshes, often increasing the growth of grass, which may cause the marsh to trap sediment more efficiently and build elevation faster. However, increased nitrogen may also decrease root growth and increase sediment microbial activity (which decomposes sediment organic carbon to carbon dioxide), causing elevation-building to slow down. It is unclear whether the addition of nitrogen affects the marsh's elevation-building rate in a positive or negative way. We found that the effect of nitrogen on elevation-building depends on location. Factors such as tidal inundation and residence time influence sediment water chemistry and, thereby, the response to excess nitrogen. Sulfide inhibits the uptake of nitrogen by plant roots and also microbial activity; thus, marsh locations with more sulfide have diminished responses to nitrogen pollution. This knowledge may be used for management of marshes at risk due to nitrogen pollution.

1. Introduction

Salt marshes rely on vertical organic carbon (OC) and mineral accretion to maintain elevation above rising sea level. If salt marsh platforms do not build elevation faster than the local rate of relative sea level rise, these ecosystems may convert to mudflat or open water. Marsh elevation may be gained either through uptake of CO_2, producing biomass that results in vertical belowground expansion, or through deposition of sediment suspended in tidal water that results in vertical surface accretion (Friedrichs & Perry, 2001). The uptake of CO_2 via gross primary production (GPP) is counterbalanced by the release of CO_2 through plant and microbial respiration (R). Net ecosystem exchange (NEE), the balance between GPP and R, determines net gain or loss of OC in the marsh due to metabolism. In addition, aboveground biomass (AGB) of

dominant macrophytes such as *Spartina alterniflora,* reduces the velocity of tidal water, causing deposition of particulates and allowing marshes to efficiently trap suspended sediments. A strong positive correlation between AGB and sediment deposition has been well established in locations with ample suspended sediment availability (Mudd et al., 2009).

Nitrogen (N) availability in salt marsh ecosystems has been increasing due to anthropogenic inputs in coastal waters (Hopkinson et al., 2012; Pardo et al., 2011), impacting salt marsh accretion mechanisms in both positive and negative ways. Because salt marsh macrophytes are often N-limited (Valiela, 2015), N fertilization may cause an increase in AGB and subsequently an increase in sediment trapping and accretion. However, fertilization may also cause belowground biomass (BGB) and root: shoot ratios to decrease (Darby & Turner, 2008), reducing belowground expansion and causing destabilization that may lead to decreased stability of the marsh platform and collapse of creek banks (Deegan et al., 2012). Furthermore, fertilization has been observed to increase CO_2 efflux from sediment and degradation of organic matter by microbial respiration (Wigand et al., 2009), which may negatively impact marsh elevation.

Although numerous fertilization studies have been performed to determine the effect of increasing N on salt marsh resilience, conflicting results suggest that the response to fertilization may vary with site-specific characteristics (Davis et al., 2017). Most fertilization studies have observed an increase in AGB in response to fertilization (Anisfeld & Hill, 2012; Darby & Turner, 2008; McFarlin et al., 2008; Mendelssohn, 1979; Morris et al., 2013; Valiela, 2015); however, the response of sediment deposition varied between increasing deposition or no response (Davis et al., 2017; Morris et al., 2013). BGB has been observed to either increase (Morris et al., 2013; Wigand et al., 2015) or decrease (Darby & Turner, 2008; Deegan et al., 2012) in response to fertilization. Several studies found that R and GPP (Wigand et al., 2009; Anisfeld & Hill, 2012; Caplan et al., 2015; Geoghegan et al., 2018; Morris & Bradley, 1999; Wang, Zhu et al., 2013, Bulseco et al., 2019) increased in response to fertilization, but the results for NEE were mixed with either no detectable response (Geoghegan et al., 2018) or an increase in net CO_2 emissions (Caplan et al., 2015; Wang, Zhu, et al., 2013).

While these conflicting results could arise from variations in the type, amount, frequency, and technique of N fertilization (Johnson et al., 2016), they may also arise from heterogeneity in the physical and chemical characteristics of the locations where experiments were performed. Elevation, which largely determines the frequency and duration of marsh tidal inundation, varies across and within salt marsh locations. Because tidal water acts as a barrier to diffusion of atmospheric oxygen into marsh sediment, inundation time may have an especially strong influence on chemical characteristics of marsh pore water. Marshes with long inundation times tend to have more reduced conditions and greater sulfide (H_2S) content (Howes & Goehringer, 1994). The residence time of pore water, which varies depending on sediment composition, slope, elevation, tidal amplitude, and groundwater hydrology (Tamborski et al., 2017), governs the concentrations of metabolic products accumulating in pore water. Creekbanks, distinct subhabitats within marsh ecosystems, often have a high elevation berm resulting from high rates of sediment deposition (Temmerman et al., 2003). Exposure to highly energic oxic creek water often rapidly flushes pore water in creek bank sediments (Gardner, 2005; Harvey et al., 1995). Thus, physical characteristics, which drive differences in inundation and pore water exchange, shape spatially heterogeneous pore water chemistry across salt marsh locations.

Contrasting pore water characteristics interact with N and C cycling in salt marshes and can alter the response of marsh biomass production and metabolism to N fertilization. H_2S, the product of sulfate reduction that accumulates to high concentrations in some marsh locations, inhibits coupled nitrification-denitrification (Burgin & Hamilton, 2007; Joye & Holibaugh, 1995), preventing heterotrophic denitrification from mineralizing OC to CO_2, whereas it may stimulate chemolithotrophic dissimilatory nitrate reduction to ammonium (DNRA) by acting as an electron donor (Burgin & Hamilton, 2007), enhancing CO_2 uptake. Because DNF is a heterotrophic process and DNRA is either chemolithotrophic or fermentative (Washbourne et al., 2011), shifting the dominance of these processes likely influences overall C cycling and responses to fertilization. H_2S is known to act as a toxin to *S. alterniflora* at high concentrations (Lamers et al., 2013), stunting biomass production and limiting GPP by inhibiting N uptake (Bradley & Morris, 1990). Release of O_2 by *S. alterniflora* roots acts as a defense against H_2S

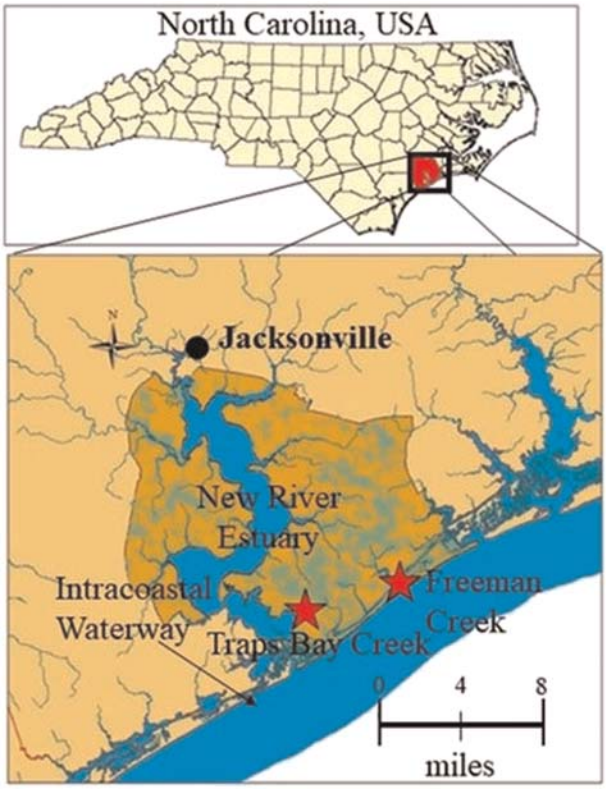

Figure 1. Map of Camp Lejeune Marine Corp Base, NC, USA (34°35′52.8″ N, 77°19′37.2″W) with the experimental plot locations marked with red stars.

toxicity by oxidizing H_2S to sulfate (Lee et al., 1999) and enhancing coupled nitrification-denitrification (Hinshaw et al., 2017).

Marsh NEE can be measured using either chambers or eddy covariance towers. For this study, we have chosen to use chambers since they easily allow for experimental manipulations such as fertilization; however, chamber measurements present a challenge due to the short time scale for measurements and labor-intensive protocols. Chamber studies typically ignore the effects of tidal inundation since they are most often performed during marsh emergence from tidal water. Since tidal water may act as a diffusion barrier to atmospheric CO_2 and O_2, affect *S. alterniflora* metabolism through stomatal closure and inhibition of photosynthesis (Pezeshki, 2001), and cause the CO_2 produced by R to dissolve as DIC, we have developed a model to extrapolate CO_2 fluxes to an annual scale that incorporates a correction for the effects of tidal inundation.

This study examined variations in responses of *S. alterniflora* biomass and ecosystem metabolism to fertilization across three marsh locations with contrasting physical characteristics. We scaled chamber measurements to annual fluxes using an extrapolation model, compared results to eddy covariance tower observations to assess differences between methods, and quantified the importance of inundation correction on our extrapolation model. We hypothesized that physical characteristics of a salt marsh drive location-specific pore water chemistry, modulating responses of biomass and metabolic rates to fertilization. Fertilization responses were expected to be greater in locations with higher elevation, lower inundation periods, and close proximity to tidal creeks, whereas in interior sites with low elevation and long inundation periods sulfide will diminish responses to fertilization.

2. Materials and Methods

2.1. Site Description

Field experiments were conducted at two tidal creek systems on Marine Corps Base Camp Lejeune, NC, USA (Figure 1, 34°35′52.8″N, 77°19′37.2″W) to represent marshes with contrasting physical characteristics (Table 1; see Figure S1 in the supporting information for detailed plot pair locations). Plots were established in both the interior marsh and along the creek edge at Freeman Creek (FC), a tidal creek bordering the Atlantic Intracoastal Waterway. The FC creek edge had a berm with an elevation 0.25 m higher than the average FC interior marsh elevation. A third site was selected in the interior of a fringing marsh near the mouth of Traps Bay Creek (TBC), a tidal creek in an embayment within the New River Estuary. The FC sites were within an extensive *S. alterniflora* –dominated marsh, while the TBC site was within a *S. alterniflora* zone that transitioned into *Juncus roemerianius* (Davis et al., 2017; McTigue et al., 2019). The tidal range averaged 0.31 m at TBC and 0.83 m at FC (Lettrich, 2011; McTigue et al., 2019). Seasonal differences in water level were greater at TBC than FC, due to the influence of freshwater inputs and wind-driven tides (Ensign et al., 2017). As a consequence, the TBC *S. alterniflora* marsh has a longer annual tidal inundation period and occupies a narrower elevation range than FC. Using the Darcy method, pore water residence times at FC and a tidal creek adjacent to TBC were estimated to be 12 and 90 days, respectively (Lettrich, 2011).

Table 1
Physical Characteristics of the Three Experimental Marsh Sites

Characteristic	Unit	FC edge	FC interior	TBC interior
Tidal amplitude[a]	m	0.83	0.83	0.31
Elevation (NAVD88)[b]	m	0.21	−0.04	0.08
Annual % time inundated[c]	%	36	55	68
Typical salinity range[d]		30–35	30–35	25–32
Pore water residence time[e]	days	Unknown	12	90
Tidal creek proximity	m	0–5	>25	>5

[a]Ensign et al. (2017). [b]Average plot elevation based on laser level measurements. [c]Based on water level data from hobo dataloggers and the NOAA Beaufort tidal gauge (which closely matched Hobo water level data at FC). [d]YSI readings in the creeks near the sites over several tidal cycles per season. [e]Lettrich (2011).

2.2. Experimental Design

Three replicate control-fertilized plot pairs were established in each of the three selected sites, maintaining at least 1 m between plots. Two

piezometers at 5 and 15 cm sediment depths and a 0.9 m × 0.9 m square aluminum collar with drainage holes were permanently installed in each plot at the beginning of the experiment. A solid mixture of NH_4NO_3 and P_2O_5 (30 mol N yr^{-1} and 15 mol P yr^{-1}) was broadcast once per season in spring, summer, fall, and winter, 2015, and spring and summer, 2016 on randomly chosen plots, which received one fourth of the annual dose per season. This fertilization rate was selected because it has been used in several other studies (Morris et al., 2002; Valiela, 2015), and is within natural levels of N enrichment on the U.S. East Coast (Wigand et al., 2009). Plots were sampled seasonally from Fall 2015 to Summer 2016 about 1 month after each fertilization.

2.3. Pore Water Chemistry

Pore water was collected seasonally from each 5 and 15 cm piezometer to measure H_2S, NH_4^+, DOC, and DIC concentrations. Piezometers were flushed with N_2 prior to sampling to remove reactive gases, and pumped to flush out stagnant pore water. The H_2S, NH_4^+, and DOC samples were filtered in the field with 0.45 μm polyethylsulfone syringe filters, and DIC samples were collected without filtering in 8 ml hungate tubes spiked with 8 μL of saturated $HgCl_2$. H_2S samples were filtered directly into 0.01 M zinc acetate solution and analyzed on a spectrophotometer using Cline's reagent (Cline, 1969) within 15 days of collection. NH_4^+ samples were stored frozen and analyzed on a Lachat Quickchem using phenol hypochlorite (Solorzano, 1969). Because H_2S in samples causes a false NH_4^+ signal using the phenate method, H_2S was removed from samples by acidifying to a pH < 3 with sulfuric acid, sparging with argon gas for 8 min, and reneutralizing using NaOH prior to analysis. DOC samples were filtered into combusted scintillation vials (500°C for 5 hr), frozen for storage, and analyzed on a Shimadzu TOC-V analyzer. DIC samples were analyzed within 30 days of collection with a Li-Cor 6252 infrared CO_2 analyzer by injecting 100 μL of sample into 0.05 M H_2SO_4 sparged with N_2 gas as described in Neubauer and Anderson (2003).

2.4. Biomass

S. alterniflora AGB was estimated seasonally inside each plot collar by measuring the height of 10 randomly selected stems to the tip of the longest leaf, and converting these heights to AGB per stem using the algorithm in Davis et al., 2017. Stem density was determined within a 0.25 m quadrat in each plot and used to scale to AGB per m^2.

BGB was measured once at the end of the experiment (November 2016) by collecting one 20 cm deep, 6.4 cm diameter sediment core from each plot, rinsing the sediment through a 1 mm pore size sieve, drying the remaining biomass at 60°C for 2 weeks, and weighing the dried biomass.

2.5. Chamber Measurements of Metabolic Rates

Vertical CO_2 fluxes in each plot were measured once per season with a Los Gatos Ultraportable Greenhouse Gas Analyzer (Model 915-0011) using static chambers equipped with an ice water cooling system to maintain chamber interiors within 2°C of ambient air temperature (Neubauer et al., 2000). A C1000 Campbell datalogger was used to log air and sediment temperatures, measured with thermocouples, and photosynthetically active radiation (PAR) determined with Li-Cor 190R Quantum deck sensors inside and outside the chambers, each at 15 s intervals. The static chambers were covered with shade cloths to measure CO_2 fluxes at four different light conditions. The flux for each light condition was measured for approximately 5–8 min, and the goodness of fit for each flux was >0.995 for CO_2 concentration readings made every 45 s. The CO_2 flux measured in the dark represented respiration (R), and the three other light levels (approximately 25%, 50%, and 100% ambient light) were used to construct photosynthesis-irradiance (P-I) curves for modeling GPP.

2.6. Scaling Observed Metabolic Rates to Daily and Annual Rates

Respiration Q_{10} was determined experimentally in triplicate 10 cm deep × 6.4 cm diameter sediment cores taken at both FC and TBC interior sites in November 2016. After overnight equilibration to the chamber temperature, cores were incubated for 12 hr at 15°C and 25°C in a dark environmental chamber at the Virginia Institute of Marine Science. Headspace samples were taken three times during incubations for determination of CO_2 concentrations using a Li-Cor 6,252 infrared gas analyzer to determine R. The formula used to calculate the Q_{10} value for each core was

Table 2
Seasonal Averages (Standard Errors) of Pore Water Analyte Concentrations

			Control						Fertilized					
	Site		Freeman Edge		Freeman Interior		Traps		Freeman Edge		Freeman Interior		Traps	
	Depth (cm)		5	15	5	15	5	15	5	15	5	15	5	15
H_2S (μM)	Fall		43 (19)	905 (88)	561 (407)	875 (437)	1,209 (112)	2,716 (263)	13 (13)	372 (240)	2,629 (1639)	1,486 (843)	1,335 (916)	2,893 (512)
	Winter		0 (0)	130 (73)	87 (70)	341 (196)	1,183 (780)	2,119 (682)	3 (3)	0 (0)	202 (149)	91 (62)	144 (92)	1808 (126)
	Spring		0 (0)	37 (37)	376 (305)	142 (101)	889 (573)	1,138 (134)	0 (0)	5 (5)	101 (69)	83 (47)	106 (60)	943 (125)
	Summer		22 (22)	711 (295)	768 (362)	544 (104)	870 (338)	2,566 (830)	0 (0)	188 (186)	810 (69)	548 (81)	642 (287)	2,501 (548)
NH_4^+ (μM)	Fall		3.8 (0.5)	14.8 (6.1)	39.6 (21.7)	94.7 (45.4)	119.8 (52.9)	329.2 (52.9)	7.0 (1.6)	11.9 (3.8)	48.7 (31.6)	71.7 (36.1)	82.4 (46.5)	654.8 (288.5)
	Winter		5.6 (1.0)	5.8 (1.7)	28.4 (9.7)	37.3 (8.0)	115.6 (64.0)	279.6 (75.5)	7.1 (3.2)	11.2 (4.2)	84.4 (29.4)	144.5 (46.7)	889.8 (807.5)	1180.9 (271.0)
	Spring		2.0 (0.6)	9.1 (3.5)	37.7 (12.8)	30.7 (9.6)	68.2 (48.2)	177.8 (71.4)	3.6 (0.7)	5.2 (2.2)	94.3 (35.6)	128.0 (70.9)	546.3 (501.2)	1196.0 (461.2)
	Summer		4.7 (0.2)	12.6 (2.3)	105.2 (11.3)	79.1 (24.2)	98.7 (78.0)	242.6 (78.6)	6.0 (0.5)	5.8 (1.4)	305.2 (145.8)	324.9 (239.2)	102.4 (70.4)	776.8 (307.9)
DIC (mM)	Fall		3.53 (0.29)	9.54 (1.40)	5.46 (1.29)	10.31 (3.87)	10.11 (1.86)	13.84 (2.26)	3.18 (0.35)	9.67 (2.25)	7.29 (2.39)	6.25 (1.74)	8.53 (2.00)	17.35 (1.24)
	Winter		2.59 (0.20)	4.80 (0.86)	3.19 (0.67)	4.54 (0.84)	7.23 (1.81)	13.88 (2.81)	3.13 (1.04)	4.62 (0.75)	4.17 (1.49)	3.17 (0.43)	3.61 (0.97)	15.49 (0.64)
	Spring		4.12 (1.15)	5.10 (0.88)	4.89 (1.30)	5.25 (0.97)	7.86 (2.68)	12.31 (1.88)	5.16 (1.08)	6.48 (0.86)	4.69 (0.67)	4.89 (0.40)	3.59 (1.10)	12.10 (1.73)
	Summer		4.17 (0.33)	8.70 (1.10)	7.32 (1.44)	9.14 (1.54)	8.54 (1.02)	13.41 (0.88)	5.51 (0.66)	9.37 (0.99)	7.01 (0.87)	9.27 (0.67)	5.89 (0.76)	13.66 (0.92)
DOC (mM)	Fall		0.25 (0.04)	0.46 (0.23)	0.54 (0.10)	0.72 (0.00)	1.19 (0.17)	1.58 (0.20)	0.24 (0.02)	0.50 (0.15)	0.62 (0.18)	0.52 (0.04)	1.21 (0.16)	1.54 (0.30)
	Winter		0.34 (0.09)	0.23 (0.13)	0.37 (0.01)	0.51 (0.01)	0.94 (0.02)	1.05 (0.16)	0.24 (0.03)	0.25 (0.02)	0.50 (0.09)	0.35 (0.01)	0.67 (0.04)	1.07 (0.05)
	Spring		0.40 (0.18)	0.55 (0.29)	0.61 (0.18)	0.91 (0.08)	1.06 (0.03)	1.41 (0.23)	0.33 (0.04)	0.29 (0.04)	0.56 (0.09)	0.32 (0.04)	0.77 (0.16)	1.35 (0.10)
	Summer		0.40 (0.08)	0.66 (0.31)	1.37 (0.46)	0.99 (0.01)	1.15 (0.30)	1.69 (0.23)	0.30 (0.03)	0.48 (0.22)	0.87 (0.25)	0.84 (0.10)	1.13 (0.25)	1.71 (0.19)

$$Q_{10} = R_2/R_1^{(10/(T2 - T1))}$$

where R_1 and R_2 correspond to rates of R measured at temperatures T1 (15°C) and T2 (25°C), respectively. Because no significant differences between Q_{10} values were detected across sites, the average of all six values was used to extrapolate R to hourly rates based on sediment temperature.

The initial slope (α) and P_{max} of P-I curves were calculated using the equation from Jassby and Platt (1976) in the phytotools package (Silsbe & Malkin, 2015) for R software (R Core Team, 2014). An exponential relationship between alpha and temperature was used to adjust daily α throughout the year. Daily P-I curves with temperature-adjusted alphas were then used to model hourly GPP using average hourly PAR from the CRONOS Database weather station at the Pamlico Aquaculture Field Laboratory in Aurora, NC (https://climate.ncsu.edu/cronos/?station=AURO). Because no clearcut relationship was observed between P_{max} and sediment temperature, P_{max} remained fixed during each season.

2.7. Correcting Modeled Hourly R and GPP for Tidal Inundation

Modeled hourly CO_2 fluxes due to R and GPP were modified based on tidal inundation depth. A previous study (Zawatski, 2018) observed that CO_2-derived R and GPP rates both decreased linearly with increasing tidal water depth, resulting in zero CO_2 flux when the water depth and the average plant height were equal. This relationship was applied to correct hourly R and GPP fluxes in each plot based on the average plant height and hourly average water depth in each plot. GPP, R, and NEE values were scaled up to daily and annual rates by summing modeled hourly values. The average hourly modeled chamber NEEs for FC interior control plots were validated by comparison to NEEs observed concurrently using an eddy covariance tower located in the interior of FC (tower data from Fogarty, 2018). The FC interior plots were within the typical tower flux footprint. Thirty days per season were compared surrounding the date of chamber measurements.

2.8. Statistics

Mixed-effect models with location, season, and treatment (fertilized vs. control) as fixed factors and a repeated measure term were performed using the lme4 package (Bates et al., 2015) in the statistical software R (R Core Team, 2014) to determine significant differences ($p < 0.05$) between treatments and locations for seasonal data. Treatment and location were used as fixed effects and plot pair as a random effect to compare end-of-experiment BGB and annual GPP, R, and NEE values. Analysis of variance (ANOVA) assumptions of normality and equal variance were tested, and to meet the normality assumption, the H_2S data were square root transformed and the NH_4^+, DIC, DOC, and AGB data were log-transformed. Tukey posthoc tests were performed for pairwise contrasts between factors.

Structural equation modeling (SEM) was used to determine direct and indirect effects of pore water chemistry and fertilization on

Table 3
Results of Mixed-Effect Models for All Variables in This Study, Including P Values and Degrees of Freedom (Df)

			Location	Treatment	Season	Location: treatment	Location: season	Treatment: season	Location:treatment: season
Pore water sulfide	5 cm depth	Df	**2**	1	**4**	2	**7**	**4**	7
		P	**5.69E−06**	0.63022	**6.68E−09**	0.12136	**5.46E−06**	**0.03414**	0.05384
	15 cm depth	Df	**2**	1	**4**	2	**7**	4	7
		P	**7.35E−07**	0.371	**1.15E−07**	0.635	**4.65E−08**	0.911	0.857
Pore water DOC	5 cm depth	Df	**2**	**1**	**3**	2	**6**	3	6
		P	**1.55E−07**	**0.017**	**2.82E−08**	0.969	**6.91E−07**	0.176	0.117
	15 cm depth	Df	**2**	**1**	**3**	2	6	**3**	6
		P	**1.57E−13**	**0.011**	**<2.2E−16**	0.104	0.559	**0.002**	0.117
Pore water NH_4^+	5 cm depth	Df	**2**	1	**4**	2	**8**	4	8
		P	**<2.20E−16**	0.100	**0.023**	0.908	**0.001**	0.098	0.646
	15 cm depth	Df	**2**	**1**	4	**2**	8	**4**	8
		P	**<2.20E−16**	**0.041**	0.098	**0.032**	0.235	**0.003**	0.212
Pore water DIC	5 cm depth	Df	2	1	**4**	**2**	**8**	4	8
		P	0.067	0.110	**8.02E−14**	**0.005**	**1.56E−06**	0.676	0.127
	15 cm depth	Df	**2**	1	**4**	2	**8**	4	8
		P	**1.08E−04**	0.891	**2.02E−11**	0.164	**2.52E−07**	0.905	0.486
Biomass	AGB	Df	**2**	**1**	3	**2**	**6**	**3**	**6**
		P	**1.60E−06**	**<2.20E−16**	0.126	**0.028**	**2.23E−06**	**0.017**	**0.020**
	Stem Density	Df	**2**	**1**	**3**	**2**	**6**	**3**	**6**
		P	**1.38E−06**	**5.33E−12**	**<2.20E−16**	**0.004**	**0.002**	**0.004**	**0.008**
	Stem Height	Df	**2**	**1**	**3**	2	**6**	3	**6**
		P	**<2.20E−16**	**<2.20E−16**	**0.006**	0.167	**3.02E−07**	0.141	**0.048**
	BGB	Df	**2**	**1**	—	**2**	—	—	—
		P	**0.001**	**0.019**	—	**0.025**	—	—	—
Annual metabolism	Annual GPP	Df	**2**	**1**	—	**2**	—	—	—
		P	**2.84E−05**	**<2.20E−16**	—	**0.004**	—	—	—
	Annual R	Df	**2**	**1**	—	**2**	—	—	—
		P	**<2.00E−16**	**<2.00E−16**	—	**0.020**	—	—	—
	Annual NEE	Df	2	**1**	—	**2**	—	—	—
		P	**0.003132**	**4.42E−08**	—	**3.68E−05**	—	—	—

Note. Bold values are statistically significant.

biomass and metabolic parameters. The piecewise SEM package (Lefcheck, 2016) was used in R software to construct and analyze SEMs. Pore water concentrations from 5 and 15 cm depths were averaged for SEM analysis.

3. Results

3.1. Pore Water Chemistry

Based on mixed-effect model analysis, each measured pore water analyte differed significantly between experimental locations (Tables 2 and 3). FC edge pore water had significantly lower concentrations of H_2S ($p = 0.002$ at 15 cm depth), NH_4^+ ($p < 0.01$ at 5 and 15 cm depths), DOC ($p = 0.001$ at 5 cm depth; $p = 1 \times 10^{-4}$ at 15 cm depth), and DIC (no difference at 5 cm depth, $p = 0.009$ at 15 cm depth) than FC interior and TBC. H_2S, DOC, and DIC concentrations in fertilized plots were not significantly different than in control plots; however, DOC at 5 cm was significantly greater in fertilized plots than control plots ($p = 0.007$).

3.2. Biomass

According to the mixed-effect model results, FC edge had significantly greater AGB per m^2 than FC interior ($p = 0.009$) and TBC ($p = 0.01$) but AGB at TBC and FC interior were not different (Figure 2a). AGB was significantly greater in fertilized plots than in control plots overall ($p = 0.0001$); however, an interaction between the treatment and location factors ($p = 0.028$) indicated that there was no significant difference between control and fertilized AGB at TBC. During summer 2016, AGB in fertilized FC edge plots peaked

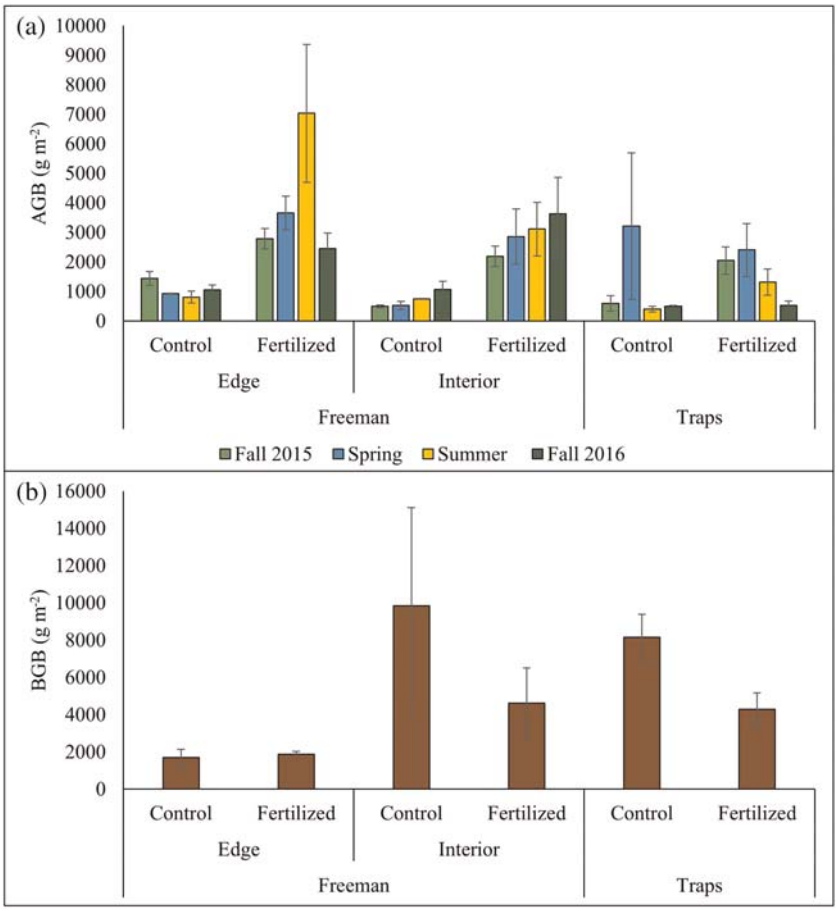

Figure 2. (a) Aboveground biomass (AGB) and (b) belowground biomass (BGB) across sites and treatments. BGB was measured only during the Fall 2016 season.

dramatically to more than double the biomass of fertilized FC interior or TBC plots. Fertilized plots had significantly greater stem density ($p = 0.002$) and stem height ($p = 0.001$) overall (Table S1); however, an interaction between location and treatment for stem density ($p = 0.004$) (but not stem height) indicated that there was no difference between control and fertilized stem density at TBC.

BGB (Figure 2b) in FC edge control plots had less than 20% the amount of BGB measured in the control plots at the other two sites ($p = 0.0001$, Figure 2b), with a fivefold lower root: shoot ratio (Table S1) than interior and TBC plots. While BGB in the FC fertilized and control plots was not different on the edge, BGB in the fertilized FC interior and TBC plots was less than 50% of the BGB in respective control plots ($p = 0.01$). The root:shoot decreased at each location in response to fertilization, as expected.

3.3. Daily NEE

Daily NEE and its response to fertilization differed depending on location (Figure S2). NEE was more dynamic and seasonally variable at FC edge control than in other treatments, ranging from −400 to +400 mmol CO_2 m^{-2} day^{-1}. FC interior control plots were more balanced at zero net daily flux throughout the year with less seasonal variation and range than the edge, and TBC was similarly balanced but shifted further toward net CO_2 uptake than FC interior in the spring. Fertilization on the FC edge caused daily NEE to become even more dynamic, especially during Fall 2015 and Spring 2016, with a clear shift toward greater daily net CO_2 emission in the winter, spring, and summer. The fertilized FC edge displayed the greatest daily net emission of the sites during summer 2016 with an emission of 400–800 mmol CO_2 m^{-2} day^{-1} and also the highest net daily uptake rates during fall 2015, as high as 800 mmol CO_2 m^{-2} day^{-1}. The fertilized FC interior also exhibited a shift toward net emission during fall and summer and a shift toward net

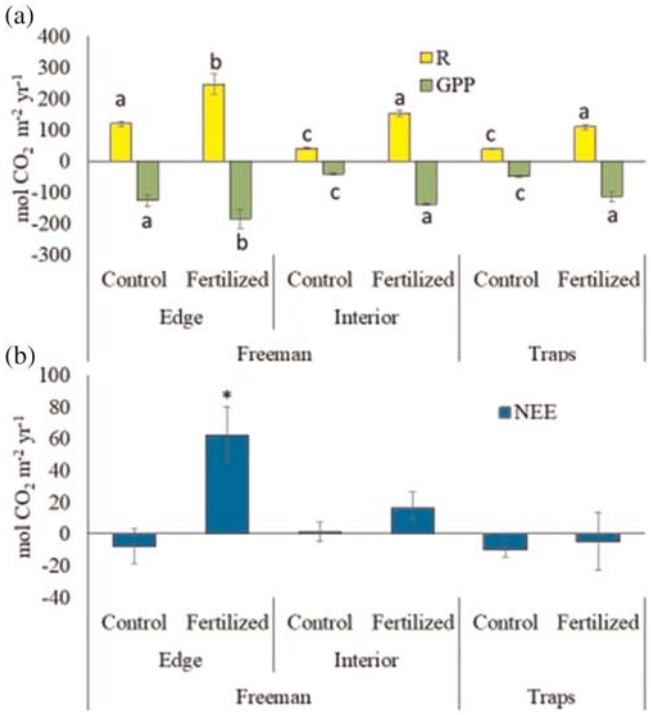

Figure 3. (a) Annual respiration (yellow), gross primary production (green) and (b) net ecosystem exchange in fertilized and control plots at the three experimental locations. Different letters on panel (a) indicate statistically different fluxes, and the asterisk on panel (b) indicates a statistically different flux. Positive values for R and NEE represent emission while negative values for GPP represent uptake.

uptake during spring. The response to fertilization at TBC was more diminished than at the other two sites, with no clear seasonality or shift toward uptake or emission overall.

3.4. Annual Metabolism

Annual GPP (Figure 3a) in control plots on the FC edge averaged 127 mol CO_2 m^{-2} yr^{-1}, more than double the GPP in control plots of the other two sites ($p = 2.8 \times 10^{-5}$), but FC interior and TBC control sites did not differ. Based on the mixed-effects model, GPP was significantly greater in fertilized plots than control plots ($p = 7.4 \times 10^{-6}$); however, an interaction between location and fertilization ($p = 0.004$) indicated that while GPP was greater in FC edge control plots than FC interior and TBC control plots, GPP in fertilized plots was not different across the three locations.

R showed a similar pattern to GPP across the sites. Annual control plot R averaged 120 mol m^{-2} yr^{-1} at FC edge, more than double the R in control plots of the two interior sites ($p < 1 \times 10^{-5}$), but the two interior sites did not differ. Based on the mixed-effects model results, R was significantly greater in fertilized plots than control plots overall ($p = 2 \times 10^{-16}$), but a significant interaction between location and treatment ($p = 0.019$) indicated that R rates in fertilized plots of the interior and TBC were not different than in control plots on the edge.

NEE (Figure 3b) was nearly balanced near net zero annual CO_2 flux at all three sites. Based on the mixed-effects model, fertilized plots had higher rates of net CO_2 emission than control plots overall ($p = 1.3 \times 10^{-11}$); however, a significant interaction between location and fertilization ($p = 3.7 \times 10^{-5}$) indicated that fertilized plots along the edge had greater annual net CO_2 emissions than edge control plots, but there were no significant differences in NEE between control and fertilized plots at FC interior and TBC. The fertilized edge plots were estimated to emit an average of 62 mol CO_2 m^{-2} $year^{-1}$.

3.5. Effect of Tidal Inundation on Vertical CO_2 Flux

The hourly modeled chamber NEE fluxes were corrected for the effect of tidal inundation based on water depth relative to the average plant height in each plot. Figure 4 displays the % reduction in annual GPP and R resulting from the inundation correction of hourly rates. On the edge, which had the highest elevation

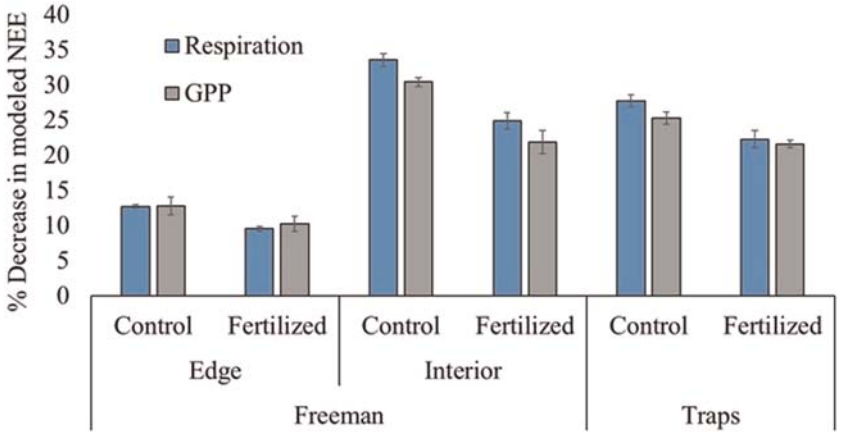

Figure 4. The % decrease in modeled R and GPP after correcting for inundation. Correction assumed a linear decrease in the flux with tidal water depth and zero flux when depth was equal to the average stem height (as observed in Zawatski, 2018).

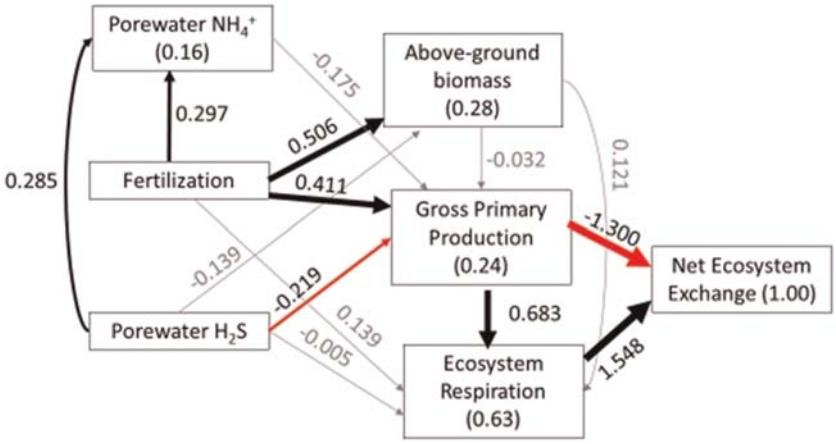

Figure 5. Structural equation model results. Gray arrows represent nonsignificant pathways, and black and red arrows indicate significant positive and negative correlations, respectively. The correlation coefficient and thickness of each arrow corresponds to the relative strength of the relationship. The value within each box represents total correlation coefficient for that variable.

and lowest % annual inundation time, both GPP and R were reduced 9–13% by the inundation correction, but because both GPP and R corrections were reduced by nearly the same magnitude, the inundation correction had a negligible effect on NEE. In the FC and TBC interiors, R and GPP were reduced by 20–35%, and because R was reduced more than GPP, the annual NEE value was offset in the direction of net uptake. The greatest reduction in net CO_2 emissions was 12 mol CO_2 per year for the fertilized FC interior plots.

3.6. Chamber Versus Tower CO_2 Measurements

Modeled hourly NEE for FC interior control plots corrected for tidal inundation were averaged and compared to hourly eddy covariance tower flux observations (Fogarty, 2018) for 30 days during each season (Figure S3). Average hourly NEE in FC interior control plots were similar in magnitude to the eddy covariance tower observations, with a root-mean-square error (RMSE) of 6.6 mmol m^{-2} hr^{-1}; however, in Fall 2015 the chamber model consistently estimated greater midday CO_2 uptake than tower measurements, while in Spring 2016 midday net CO_2 uptake observed by the tower was at least double the NEE modeled by chamber measurements for 8 of the 30 days. A linear regression comparing the methods (Figure S4) indicates that, while positively correlated, modeled chamber NEE tended to be greater than tower NEE.

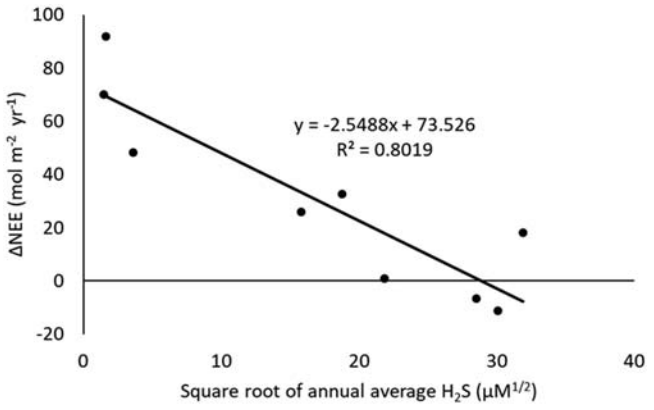

Figure 6. The relationship between annual average pore water H_2S concentration (square root transformed) and the response of annual NEE to fertilization ($p = 0.009$). ΔNEE = (NEE in fertilized plot) − (NEE in control plot) for each plot pair.

3.7. Structural Equation Model

A SEM with the structure presented in Figure 5 had an AIC score of 59 and overall p value of 0.516 (models above $p = 0.05$ were considered significant). Fertilization and pore water H_2S were the only two independent variables in the model. H_2S was positively correlated with pore water NH_4^+ but negatively correlated with GPP; however, pore water H_2S was not correlated with AGB and R. Fertilization was positively correlated with pore water NH_4^+, AGB, and GPP but was not directly correlated with R. GPP and R were strongly positively correlated, and both GPP and R had strong but opposing correlations with NEE. AGB was not directly correlated with the rates of GPP or R.

The interaction of H_2S concentrations with the response of NEE to fertilization, which was implied by the results of the SEM, was visualized with a linear regression of the square root of average H_2S concentrations versus the difference in NEE between each control and fertilized plot pair (Figure 5). This resulted in a significant negative linear relationship ($p = 0.009$) with an R^2 value of 0.80, suggesting that accumulation of H_2S in pore water reduces the impacts of marsh fertilization on NEE (Figure 6).

4. Discussion

4.1. Pore Water Chemistry

The gradient of pore water H_2S, NH_4^+, DOC, and DIC concentrations observed across the three experimental locations in this study likely resulted from a combination of hydrological and biological (plant and microbial) drivers; however, the higher concentrations of GPP products (DOC) and respiration products (DIC, H_2S, and NH_4^+) observed at sites with lower rates of GPP and R suggests that physical variables played a more import role than biological process rates in regulating pore water characteristics. Longer pore water residence and inundation times at TBC were the likely cause for the greater accumulation of pore water analytes at TBC. Because tidal water acts as a diffusion barrier blocking exposure of marsh sediments to oxygen, marshes with longer duration and frequency of inundation tend to have sediments with more reduced conditions and greater H_2S concentrations (DeLaune et al., 1983; Wigand et al., 2016). The lower concentrations of analytes on FC edge were expected due to more rapid pore water drainage and flushing of the pore space with oxic creek water (Howes & Goehringer, 1994; King et al., 1982). At TBC, pore water H_2S frequently exceeded 2 mM, the threshold experimentally determined to completely inhibit N uptake by *S. alterniflora* (Bradley & Morris, 1990); thus, the observed H_2S concentrations were within a relevant range to impact *S. alterniflora* metabolism.

The fate of N fertilizer differed among sites. At FC edge and interior, potential fates of NH_4^+ included uptake by *S. alterniflora*, microbial nitrification, or export due to flushing (Pastore et al., 2016), The high H_2S at TBC likely inhibited *S. alterniflora* N uptake and microbial nitrification (Joye & Hollibaugh, 1995); thus, the NH_4^+ added by fertilization accumulated in pore water to a much greater extent at TBC than at the other sites with lower H_2S.

4.2. Biomass

AGB was lower at the TBC site than at the FC sites, likely because aboveground growth was stunted by H_2S inhibition of N uptake. As expected in a marsh with N limitation of plant growth, fertilization resulted in greater stem density, stem heights, and AGB at both FC edge and interior; however, at TBC stem density and AGB were not affected by fertilization. The lack of a response at TBC despite the presence of excess pore water N suggests that growth of *S. alterniflora* at TBC was not limited by N availability but by the rate of N uptake. Currently, a small minority of other studies have similarly observed a lack of response of AGB to fertilization (Davis et al., 2017; Johnson et al., 2016). As observed in this and other studies, sediment deposition increases with AGB (Morris et al., 2002); thus, pore water chemistry, by modulating the response of AGB to fertilization, also potentially controls the response of sediment accretion rates to fertilization.

BGB showed varying responses to fertilization across the three locations. BGB in FC edge did not respond to fertilization, but at both interior sites BGB decreased with fertilization. Fertilizing interior marsh sites caused *S. alterniflora* to shift the partitioning of fixed C from BGB to AGB, which may decrease net surface elevation gain. A previous study conducted in the FC interior using $(NH_4)_2SO_4$ as fertilizer (Davis et al., 2017), rather than NH_4NO_3 as in this study, found that BGB did not respond to fertilization. Thus, the type of fertilizer applied may lead to different responses of BGB in the same location.

4.3. Vertical Carbon Fluxes

4.3.1. Metabolic Rates

Rates of NEE varied daily between autotrophy and hetrotrophy, but patterns differed across seasons and locations. FC edge with a greater magnitude of R and GPP demonstrated more dynamic variations in daily NEE relative to those in interior sites. On an annual scale, NEE was similar across the three study locations, nearly balanced between net CO_2 emission and uptake (Figure 2). Differences in the variation of daily NEE across locations, especially in the spring and summer, did not lead to significant differences in the response of the annual flux. However, the differences in daily NEE's response to fertilization across locations resulted in significantly greater annual CO_2 emissions on the fertilized edge than in the interior marsh sites.

While both annual GPP and R varied across locations, within locations GPP and R in control plots were consistently similar in magnitude, with a nearly balanced NEE, demonstrating that R is closely coupled to the

products of GPP in these salt marshes. Coupling of GPP and R has been observed in other ecosystems such as sea grass beds (Duarte et al., 2010) and forests (Fernandez-Martinez et al., 2014), and may result from stimulation of plant R by increased *S. alterniflora* biomass as well as increase of microbial R due to the release of O_2 and labile carbon from roots (Lee et al., 1999).

Although the C sequestration capabilities of salt marsh ecosystems result from high primary production (Burden et al., 2013; Drake et al., 2015), causing them to be effective sinks for "blue" carbon (McLeod et al., 2011), R and GPP were closely in balance in this study. Average salt marsh NEE on the Atlantic coast has recently been reported to take up 19 ± 7 mol C m^{-2} $year^{-1}$ (Windham-Myers et al., 2018); sites that were net heterotrophic were considered outliers and not included in this average. However, a growing number of studies have shown marshes to be net sources of CO_2 (Krauss et al., 2016; Wang et al., 2017; Wilson et al., 2015), raising questions regarding the origin of the OC respired. In salt marshes, OC is produced by autochthonous primary production but may also be delivered via sediment deposition during tidal flooding. Allochthonous sediment OC may fuel microbial respiration, resulting in balanced NEE even when there is also sequestration of OC in buried plant biomass. Marshes with balanced NEE may continue to sequester C and maintain elevation above sea level via accretion of sediment from tidal waters (Kirwan & Murray, 2007). The elevation of Freeman interior has been observed to increase 0.2 to 1.2 cm $year^{-1}$ (Davis et al., 2017), suggesting that sediment deposition drives accretion rates at Freeman Creek marsh. Ensign and Currin (2017) determined that suspended sediment concentrations in the FC marsh during tidal flooding were consistent from the creekbank to the interior marsh and that resuspension of the sediment surface microlayer delivered substantial amounts of sediment to the interior marsh.

Fertilization caused both annual GPP and R to increase at each site, but net CO_2 emissions increased only along FC edge. This loss of 62 mol C m^{-2} $year^{-1}$ along the fertilized edge is significant and could result in a decrease in overall accretion rates and elevation. Other salt marsh studies have similarly concluded that fertilization increases both GPP and R (Anisfeld & Hill, 2012; Caplan et al., 2015; Geoghegan et al., 2018; Martin et al., 2018; Morris & Bradley, 1999; Wang, Zhu et al., 2013); however, studies are less congruent about the effect of fertilization on NEE, showing variation between no detectable effect (Geoghegan et al., 2018) and increasing CO_2 emissions (Caplan et al., 2015; Wang, Zhu et al., 2013). A decrease in soil carbon content has been observed with fertilization (Morris & Bradley, 1999) but may be a result of increased sediment input changing sediment composition rather than loss of carbon in sediment (Morris et al., 2002). Whereas results of this study suggest that sulfide is a primary driver responsible for differences across sites, other site-specific variations including hydraulic conductivity, pore water residence time, and composition of the fertilizer may explain inconsistencies observed in other studies.

4.3.2. Effects of Inundation

Great interest has recently been directed toward understanding the effect of tidal inundation on vertical carbon fluxes. Kathilankal et al., 2008 observed a reduction of midday NEE by a wide range (3–91%) during inundation. Moffett et al. (2010) observed a depth-dependent suppression of CO_2 fluxes similar to the relationship found by Zawatski (2018), which was used to correct the fluxes in this study. A study conducted in a high marsh in Massachusetts (Forbrich & Giblin, 2015) showed that inundation reduced annual NEE by about 2–4% but hypothesized that the effect of inundation would be greater in lower elevation marshes. In this present study, R and GPP were reduced by up to 13% on the less frequently inundated edge and reduced by 20–35% in the more frequently inundated FC interior and TBC marshes. While the inundation correction did not alter the annual NEE calculation at FC edge, inundation did have a significant effect on NEE calculations in the interior marshes (Table S2). Therefore, it is critical to correct NEE for the effect of inundation in low-elevation marshes when extrapolating chamber measurements to longer timescales.

4.3.3. Comparison of NEE Measured by Chambers and Eddy Covariance

Numerous studies have scaled chamber flux measurements to seasonal or annual fluxes (Anisfeld & Hill, 2012; Neubauer, 2013; Weston et al., 2014); however, the availability of an additional source of data to validate chamber extrapolation models is rare. An eddy covariance tower located at FC interior provided the opportunity to validate the chamber extrapolation model for hourly NEE in FC interior control plots. To our knowledge, only one other study (Krauss et al., 2016) has compared chamber measurement extrapolations with eddy covariance tower observations in salt marsh ecosystems. Whereas eddy covariance towers have the benefit of being a high-frequency data source, calculating tower fluxes relies on

a host of assumptions (Baldocchi et al., 1988) not applicable to chamber measurements. Chambers may be more useful for measuring small-scale spatial heterogeneity and to tease apart mechanisms driving spatial heterogeneity of gas fluxes using experimental manipulations. Greater knowledge of these mechanisms may be used to improve scaling flux estimates to whole marsh systems. While comparing the two methods may improve confidence in scaling chamber measurements, one should not expect individual plot metabolism to precisely match tower observations because the eddy covariance tower measurements reflect a larger spatial scale. Spatial heterogeneity at a smaller scale may cause individual plots to deviate from the average marsh tower footprint flux. Furthermore, the boundaries of the footprint integrated by the tower shift over time as wind speed and direction change (Baldocchi, 1997) and may capture the vertical CO_2 flux of areas not included in chamber plots, including parts of the adjacent high marsh and tidal creek.

Despite these differences between chamber and tower measurements, the average of the three FC interior control plots reflected the tower data reasonably well, indicating that the plots were representative of the whole interior marsh, and that the chamber extrapolation model was suitable for calculating daily and annual CO_2 flux values over the experimental period. Wind speed was negatively correlated with tower CO_2 flux error (Hollinger & Richardson, 2005) and, thus, nighttime, with lower wind speeds (Peltola et al., 2015), may produce greater tower error, partially explaining the slight decoupling of tower and chamber measurements at night and on days with lower wind speeds. However, nighttime decoupling could also be the result of extrapolating R measured during the day to nighttime in the chambers, assuming no diel variability in *S. alterniflora* respiration. Other studies similarly have observed minor differences in magnitude of chamber and tower flux measurements with a slight bias toward greater CO_2 fluxes from chambers than towers (Krauss et al., 2016; Poyda et al., 2017; Wang, Liu, et al., 2013) (Figure S4).

4.4. Drivers of Observed Spatial Patterns

SEM analysis proved to be useful for teasing apart direct and indirect effects of measured variables on NEE. Pore water H_2S and fertilization both positively influenced pore water NH_4^+ concentrations. Although H_2S had a direct negative effect on GPP, NH_4^+ had no effect even though they covary in concentration. These modeled results support the hypothesis that H_2S drives spatial variation in GPP and plant biomass by limiting N uptake and causing NH_4^+ to accumulate in pore water. Fertilization had a direct positive influence on both AGB and GPP; however, surprisingly, its influence on R was indrect. SEM results suggest that R is controlled primarily by variations in GPP rather than by direct inhibition by H_2S or direct stimulation by fertilization. Therefore, while fertilization has been shown to increase the rate of denitrification (Koop-Jakobsen & Giblin, 2010), a heterotrophic respiratory process, the stimulation of R by fertilization is primarily through the stimulation of plant GPP.

4.5. Implications

About 80% of the variation in the response of NEE to fertilization was explained by pore water H_2S concentrations, indicating that pore water H_2S concentrations may be a useful predictor of the relative impact of nitrogen enrichment on NEE. Highly sulfidic marshes, which tend to be those with low elevation, long inundation and residence times, and limited pore water exchange, may be more resilient to the negative impacts of increasing N availability, but they may also not benefit from the positive impacts of fertilization resulting from increased AGB and sediment deposition. Fertilized marshes with low H_2S may lose C through metabolic processes, but this loss may be balanced by increased deposition of sediment OC (Graham & Mendelsshon, 2014).

5. Conclusions

- Correcting the chamber CO_2 flux extrapolation model for the effects of tidal inundation on CO_2 fluxes was critical to avoid overestimation of annual R, GPP, and net CO_2 emission.
- The magnitude of corrected hourly NEE from chamber measurements was comparable to eddy covariance tower observations at the same site.
- Site-specific pore water H_2S, NH_4^+, DIC, and DOC concentrations were influenced by inundation time, creek proximity, and pore water residence time
- Control plots with high pore water H_2S exhibited decreased AGB, R, and GPP; however, NEE was similar and nearly balanced across all sites.

- The response of fertilization is related to location-specific pore water H_2S concentrations governed by physical characteristics.

Conflict of Interest

The authors are not aware of any conflicts of interest regarding this manuscript.

Data Availability Statement

Raw data used in this study and other DCERP data products are accessible via the DOE Environmental Systems Science Data Infrastructure for a Virtual Ecosystem (ESS-Dive, https://data.ess-dive.lbl.gov/view/doi:10.15485/1602783).

Acknowledgments

This research was conducted under the Defense Coastal/Estuarine Research Program (DCERP), funded by the Strategic Environmental Research and Development Program (SERDP). Views, opinions, and/or findings contained in this report are those of the authors and should not be construed as an official U.S. Department of Defense position or decision unless so designated by other official documentation. The authors worked in collaboration with our colleagues in the NOAA Beaufort lab, including, Jenny Davis, Nathan McTigue, Anna Hilting, Quentin Walker, Mike Greene, and Luke Snedaker, who provided the use of the greenhouse gas analyzer, performed the seasonal plot fertilizations, gathered and QC'd water level data, and installed marsh boardwalks. Many thanks to Susan Cohen, our liaison to the Marine Corps Base Camp Lejeune. This study could not have been done without Hunter Walker, who contributed much assistance including pore water nutrient analysis, building parts of the static chamber system, driving the boat to the site, and helping sample during every field campaign. Many thanks to others who helped with seasonal field campaigns: Jen Stanhope, Miguel Semedo, Shanna Williamson, Bryce Van Dam, and Scott Ensign. Thanks also to Craig Tobias and Michelle Fogarty for providing eddy covariance tower observations, Mark Brush for chamber flux modeling suggestions, and Bongkeun Song, Anne Giblin, Ellen Herbert, Annie Murphy, and Ashley Smyth for their many helpful suggestions that improved this manuscript. This is Contribution No. 3937 of the Virginia Institute of Marine Science, William & Mary

References

Anisfeld, S. C., & Hill, T. D. (2012). Fertilization effects on elevation change and belowground carbon balance in a Long Island Sound tidal marsh. *Estuaries and Coasts*, *35*(1), 201–211. https://doi.org/10.1007/s12237-011-9440-4

Baldocchi, D., Hicks, B., & Meyers, T. (1988). Measuring biosphere-atmosphere exchanges of biologically related gases with micrometeorological methods. *Ecology*, *69*, 1331–1340. https://doi.org/10.2307/1941631

Baldocchi, D. D. (1997). Flux footprints within and over forest canopies. *Boundary-Layer Meteorology*, *85*, 273–297. https://doi.org/10.1023/A:1000472717236

Bates, D., Maechler, M., Bolker, B., & Walker, S. (2015). Fitting linear mixed-effects models using lme4. *Journal of Statistical Software*, *67*(1), 1–48. https://doi.org/10.18637/jss.v067.i01

Bradley, P. M., & Morris, J. T. (1990). Influence of oxygen and sulfide concentration on nitrogen uptake kinetics in. *Spartina alterniflora*. *Ecology*, *71*(1), 282–287. https://doi.org/10.2307/1940267

Bulseco, A. N., Giblin, A. E., Tucker, J., Murphy, A. E., Sanderman, J., Hiller-Bittrolff, K., & Bowen, J. L. (2019). Nitrate addition stimulates microbial decomposition of organic matter in salt marsh sediments. *Global Change Biology*, *25*(10), 3224–3241. https://doi.org/10.1111/gcb.14726

Burden, A., Garbutt, R. A., Evans, C. D., & Jones, D. L. (2013). Carbon sequestration and biogeochemical cycling in a saltmarsh subject to coastal managed realignment. *Estuarine, Coastal and Shelf Science*, *120*, 12–20. https://doi.org/10.1016/j.ecss.2013.01.014

Burgin, A. J., & Hamilton, S. K. (2007). Have we overemphasized the role of denitrification in aquatic ecosystems? A review of nitrate removal pathways. *Frontiers in Ecology and the Environment*, *5*(2), 89–96. https://doi.org/10.1890/1540-9295(2007)5[89:HWOTRO]2.0.CO;2

Caplan, J. S., Hager, R. N., Megonigal, J. P., & Mozdzer, T. J. (2015). Global change accelerates carbon assimilation by a wetland ecosystem engineer. *Environmental Research Letters*, *10*(11), 115006. https://doi.org/10.1088/1748-9326/10/11/115006

Cline, J. D. (1969). Spectrophotometric determination of hydrogen sulfide in natural waters. *Limnology and Oceanography*, *14*(3), 454–458. https://doi.org/10.4319/lo.1969.14.3.0454

Core Team, R. (2014). *R: A language and environment for statistical computing*. Vienna, Austria: R Foundation for Statistical Computing. URL http://www.R-project.org/

Darby, F. A., & Turner, R. E. (2008). Effects of eutrophication on salt marsh root and rhizome biomass accumulation. *Marine Ecology Progress Series*, *363*, 63–70. https://doi.org/10.3354/meps07423

Davis, J., Currin, C., & Morris, J. T. (2017). Impacts of fertilization and tidal inundation on elevation change in microtidal, low relief salt marshes. *Estuaries and Coasts*, *40*(6), 1677–1687. https://doi.org/10.1007/s12237-017-0251-0

Deegan, L. A., Johnson, D. S., Warren, R. S., Peterson, B. J., Fleeger, J. W., Fagherazzi, S., & Wollheim, W. M. (2012). Coastal eutrophication as a driver of salt marsh loss. *Nature*, *490*(7420), 388–392. https://doi.org/10.1038/nature11533

DeLaune, R. D., Smith, C. J., & Patrick, W. H. Jr. (1983). Relationship of marsh elevation, redox potential, and Spartina alterniflora productivity. *Soil Science Society of America Journal*, *47*(5), 930–935. https://doi.org/10.2136/sssaj1983.03615995004700050018x

Drake, K., Halifax, H., Adamowicz, S. C., & Craft, C. (2015). Carbon sequestration in tidal salt marsh of the northeast United States. *Environmental Management*, *56*(4), 998–1008. https://doi.org/10.1007/s00267-015-0568-z

Ensign, S., & Currin, C. (2017). Geomorphic implications of particle movement by water surface tension in a salt marsh. *Wetlands*, *32*, 245–256. https://doi.org/10.1007/s13157-016-0862-4

Ensign, S., Currin, C., Piehler, M., & Tobias, C. (2017). A method for using shoreline morphology to predict suspended sediment concentration in tidal creeks. *Geomorphology*, *276*, 280–288. https://doi.org/10.1016/j.geomorph.2016.09.036

Fernandez-Martinez, M., Vicca, S., Janssens, A., Sardans, J., Luyssaert, S., Campioli, M., et al. (2014). Nutrient availability as the key regulator of global forest carbon balance. (2014). *Nature Climate Change*, *4*, 471–476. https://doi.org/10.1038/NCLIMATE2177

Fogarty, M. (2018). *Air-sea momentum, heat, and carbon dioxide fluxes in shallow coastal ecosystems Ph.D. dissertation*. Storrs, CT: University of Connecticut. https://opencommons.uconn.edu/dissertations/1766/

Forbrich, I., & Giblin, A. E. (2015). Marsh-atmosphere CO_2 exchange in a New England salt marsh. *Journal of Geophysical Research: Biogeosciences*, *120*, 1825–1838. https://doi.org/10.1002/2015JG003044

Friedrichs, C. T., & Perry, J. E. (2001). Tidal salt marsh morphodynamics: A synthesis. *Journal of Coastal Research*, *27*, 7–37. https://doi.org/10.2307/25736162

Gardner, L. R. (2005). A modeling study of the dynamics of pore water seepage from intertidal marsh sediments. *Estuarine, Coastal and Shelf Science*, *62*(4), 691–698. https://doi.org/10.1016/j.ecss.2004.10.005

Geoghegan, E. K., Caplan, J. S., Leech, F. N., Weber, P. E., Bauer, C. E., & Mozdzer, T. J. (2018). Nitrogen enrichment alters carbon fluxes in a New England salt marsh. *Ecosystem Health and Sustainability*, *4*(11), 277–287. https://doi.org/10.1080/20964129.2018.1532772

Graham, S. A., & Mendelsshon, I. A. (2014). Coastal wetland stability maintained through counterbalancing accretionary responses to chronic nutrient enrichment. *Ecology*, *95*(12), 3271–3283. https://doi.org/10.1890/14-0196.1

Harvey, J. W., Chambers, R. M., & Hoelscher, J. R. (1995). Preferential flow and segregation of porewater solutes in wetland sediment. *Estuaries*, *18*(4), 568–578. https://doi.org/10.2307/1352377

Hinshaw, S. E., Tatariw, C., Flournoy, N., Kleinhuizen, A., Taylor, C., Sobecky, P. A., & Mortazavi, B. (2017). Vegetation loss decreases salt marsh denitrification capacity: Implications for marsh erosion. *Environmental Science & Technology*, *51*(15), 8245–8253. https://doi.org/10.1021/acs.est.7b00618

Hollinger, D. Y., & Richardson, A. D. (2005). Uncertainty in eddy covariance measurements and its application to physiological models. *Tree Physiology*, *25*(7), 873–885. https://doi.org/10.1093/treephys/25.7.873

Hopkinson, C. S., Cai, W. J., & Hu, X. (2012). Carbon sequestration in wetland dominated coastal systems—A global sink of rapidly diminishing magnitude. *Current Opinion in Environmental Sustainability*, *4*(2), 186–194. https://doi.org/10.1016/j.cosust.2012.03.005

Howes, B. L., & Goehringer, D. D. (1994). Porewater drainage and dissolved organic carbon and nutrient losses through the intertidal creekbanks of a New England salt marsh. *Marine Ecology Progress Series*, *114*(3), 289–301. https://doi.org/10.3354/meps114289

Jassby, A. D., & Platt, T. (1976). Mathematical formulation of the relationship between photosynthesis and light for phytoplankton. *Limnology and Oceanography*, *21*(4), 540–547. https://doi.org/10.4319/lo.1976.21.4.0540

Johnson, D. S., Warren, R. S., Deegan, L. A., & Mozdzer, T. J. (2016). Saltmarsh plant responses to eutrophication. *Ecological Applications*, *26*(8), 2649–2661. https://doi.org/10.1002/eap.1402

Joye, S. B., & Holibaugh, J. T. (1995). Influence of sulfide inhibition of nitrification on nitrogen regeneration in sediments. *Science*, *270*, 623–625. https://doi.org/10.1126/science.270.5236.623

Kathilankal, J. C., Mozdzer, T. J., Fuentes, J. D., D'Odorico, P., McGlathery, K. J., & Zieman, J. C. (2008). Tidal influences on carbon assimilation by a salt marsh. *Environmental Research Letters*, *3*, 044010. https://doi.org/10.1088/1748-9326/3/4/044010

King, G. M., Klug, M. J., Wiegert, R. G., & Chalmers, A. G. (1982). Relation of soil water movement and sulfide concentration to *Spartina alterniflora* production in a Georgia salt marsh. *Science*, *218*(4567), 61–63. https://doi.org/10.1126/science.218.4567.61

Kirwan, M. L., & Murray, A. B. (2007). A coupled geomorphic and ecological model of tidal marsh evolution. *Proceedings of the National Academy of Sciences of the United States of America*, *104*, 6118–6122. https://doi.org/10.1073/pnas.0700958104

Koop-Jakobsen, K., & Giblin, A. E. (2010). The effect of increased nitrate loading on nitrate reduction via denitrification and DNRA in salt marsh sediments. *Limnology and Oceanography*, *55*(2), 789–802. https://doi.org/10.4319/lo.2010.55.2.0789

Krauss, K. W., Holm, G. O. Jr., Perez, B. C., McWhorter, D. E., Cormier, N., Moss, R. F., et al. (2016). Component greenhouse gas fluxes and radiative balance from two deltaic marshes in Louisiana: Pairing chamber techniques and eddy covariance. *Journal of Geophysical Research: Biogeosciences*, *121*, 1503–1521. https://doi.org/10.1002/2015JG003224

Lamers, L. P. M., Govers, L. L., Janssen, I. C. J., Geurts, J. J. M., Van der Welle, M. E. W., Van Katwijk, M. M., et al. (2013). Sulfide as a soil phytotoxin—A review. *Frontiers in Plant Science*, *4*, 268. https://doi.org/10.3389/fpls.2013.00268

Lee, R. W., Kraus, D. W., & Doeller, J. E. (1999). Oxidation of sulfide by *Spartina alterniflora* roots. *Limnology and Oceanography*, *44*(4), 1155–1159. https://doi.org/10.4319/lo.1999.44.4.1155

Lefcheck, J. (2016). PiecewiseSEM: Piecewise structural equation modelling in R for ecology, evolution, and systematics. *Methods in Ecology and Evolution*, *7*(5), 573–579. https://doi.org/10.1111/2041-210X.12512

Lettrich, M. (2011). *Nitrogen advection and denitrification loss in southeastern North Carolina salt marshes. Master's thesis*. Wilmington, NC: University of North Carolina.

Duarte, C. M., Marba, N., Gacia, E., Fourqurean, J. W., Beggins, J., Barron, C., & Apostolaki, E. (2010). Seagrass community metabolism: Assessing the carbon sink capacity of seagrass meadows. *Global Biogeochemical Cycles*, *24*, GB4032. https://doi.org/10.1029/2010GB003793

Martin, R. M., Wigand, C., Elmstrom, E., Lloret, J., & Valiela, I. (2018). Long-term nutrient addition increases respiration and nitrous oxide emissions in a New England salt marsh. *Ecology and Evolution*, *8*(10), 4958–4966. https://doi.org/10.1002/ece3.3955

McFarlin, C. R., Brewer, J. S., Buck, T. L., & Pennings, S. C. (2008). Impacts of fertilization on a salt marsh food web in Georgia. *Estuaries and Coasts*, *31*, 313–325. https://doi.org/10.1007/s12237-008-9036-9

McLeod, E., Chmura, G. L., Bouillon, S., Salm, R., Bjork, M., Duarte, C. M., et al. (2011). A blueprint for blue carbon: Toward an improved understanding of the role of vegetated coastal habitats in sequestering CO_2. *Frontiers of Ecology and the Environment*, *9*(10), 552–560. https://doi.org/10.1890/110004

McTigue, N., Davis, J., Rodriguez, A. B., McKee, B., Atencio, A., & Currin, C. (2019). Sea Level Rise Explains Changing Carbon Accumulation Rates in a Salt Marsh Over the Past Two Millennia. *Journal of Geophysical Research: Biogeosciences*, *124*(10), 2945–2957. http://doi.org/10.1029/2019jg005207

Mendelssohn, I. A. (1979). Influence of nitrogen level, form, and application method on the growth-response of *Spartina alterniflora* in North Carolina. *Estuaries*, *2*, 106–112. https://doi.org/10.2307/1351634

Moffett, K. B., Wolf, A., Berry, J. A., & Gorelick, S. M. (2010). Salt marsh-atmosphere exchange of energy, water vapor, and carbon dioxide: Effects of tidal flooding and biophysical controls. *Water Resources Research*, *46*, W10525. https://doi.org/10.1029/2009WR009041

Morris, J. T., & Bradley, P. M. (1999). Effects of nutrient loading on the carbon balance of coastal wetland sediments. *Limnology and Oceanography*, *44*(3), 699–702. https://doi.org/10.4319/lo.1999.44.3.0699

Morris, J. T., Sundareshwar, P. V., Nietch, C. T., Kjerfve, B., & Cahoon, D. R. (2002). Responses of coastal wetlands to rising sea level. *Ecology*, *83*, 2869–2877. https://doi.org/10.1890/0012-9658(2002)083[2869:ROCWTR]2.0.CO;2

Morris, J. T., Sundberg, K., & Hopkinson, C. S. (2013). Salt marsh primary production and its responses to relative sea level and nutrients in estuaries at Plum Island, Massachusetts, and North Inlet, South Carolina, USA. *Oceanography*, *26*(3), 78–84. https://doi.org/10.5670/oceanog.2013.48

Mudd, S. M., Howell, S. M., & Morris, J. T. (2009). Impact of dynamic feedbacks between sedimentation, sea-level rise, and biomass production on near-surface marsh stratigraphy and carbon accumulation. *Estuarine, Coastal and Shelf Science*, *82*, 377–389. https://doi.org/10.1016/j.ecss.2009.01.028

Neubauer, S. C. (2013). Ecosystem responses of a tidal freshwater marsh experiencing saltwater intrusion and altered hydrology. *Estuaries and Coasts*, *36*(3), 491–507. https://doi.org/10.1007/s12237-01109455-x

Neubauer, S. C., & Anderson, I. C. (2003). Transport of dissolved inorganic carbon from a tidal freshwater marsh to the York River estuary. *Limnology and Oceanography*, *48*(1), 299–307. https://doi.org/10.4319/lo.2003.48.1.0299

Neubauer, S. C., Miller, W. D., & Anderson, I. C. (2000). Carbon cycling in a tidal freshwater marsh ecosystem: A gas flux study. *Marine Ecology Progress Series*, *199*, 13–30. https://doi.org/10.3354/meps199013

Pardo, L. H., Fenn, M. E., Goodale, C. L., Geiser, L. H., Driscoll, C. T., Allen, E. B., et al. (2011). Effects of nitrogen deposition and empirical nitrogen critical loads for ecoregions of the United States. *Ecological Applications*, *21*(8), 3049–3082. https://doi.org/10.1890/10-2341.1

Pastore, M. A., Megonigal, J. P., & Langley, J. A. (2016). Elevated CO_2 promotes long-term nitrogen accumulation only in combination with nitrogen addition. *Global Change Biology*, *22*(1), 391–403. https://doi.org/10.1111/gcb.13112

Peltola, O., Hensen, A., Marchesini, L. B., Helfter, C., Bosveld, F. C., van den Bulk, W. C. M., et al. (2015). Studying the spatial variability of methane flux with five eddy covariance towers of varying height. *Agricultural and Forest Meteorology*, *214–215*, 456–472. https://doi.org/10.1016/j.agrformet.2015.09.007

Pezeshki, S. R. (2001). Wetland plant responses to soil flooding. *Environmental and Experimental Botany*, *46*, 299–312. https://doi.org/10.1016/S0098-8472(01)00107-1

Poyda, A., Reinsch, T., Skinner, R. H., Klub, C., Loges, R., & Taube, F. (2017). Comparing chamber and eddy covariance based net ecosystem CO_2 exchange of fen soils. *Journal of Plant Nutrition and Soil Science*, *180*(2), 252–266. https://doi.org/10.1002/jpln.201600447

Silsbe, G. M., & Malkin, S. M. (2015). *Phytotools: Phytoplankton production tools*. https://CRAN.R-project.org/package-phytotools

Solorzano, L. (1969). Determination of ammonia in natural waters by the phenol hypochlorite method. *Limnology and Oceanography*, *14*, 799–801. https://doi.org/10.1371/journal.pone.0066109

Tamborski, J. J., Cochran, J. K., Heilbrun, C., Rafferty, P., Fitzgerald, P., Zhu, Q., & Salazar, C. (2017). Investigation of pore water residence times and drainage velocities in salt marshes using short-lived radium isotopes. *Marine Chemistry*, *196*, 107–115. https://doi.org/10.1016/j.marchem.2017.08.007

Temmerman, S., Govers, G., Wartel, S., & Meire, P. (2003). Spatial and temporal factors controlling short-term sedimentation in a salt and freshwater tidal marsh, Scheldt estuary, Belgium, SW Netherlands. *Earth Surface Processes and Landforms*, *28*(7), 739–755. https://doi.org/10.1002/esp.495

Valiela, I. (2015). The Great Sippewissett salt marsh plots—Some history, highlights, and contrails from a long-term study. *Estuaries and Coasts*, *38*(4), 1099–1120. https://doi.org/10.1007/s12237-015-9976-9

Wang, J., Zhu, T., Ni, H., Zhong, H., Fu, X., & Wang, J. (2013). Effects of elevated CO_2 and nitrogen deposition on ecosystem carbon fluxes on the Sanjiang plain wetland in Northeast China. *PLoS ONE*, *8*(6), e66563. https://doi.org/10.1371/journal.pone.0066563

Wang, K., Liu, C., Zheng, X., Pihalatie, M., Li, B., Haapanala, S., et al. (2013). Comparison between eddy covariance and automatic chamber techniques for measuring net ecosystem exchange of carbon dioxide in cotton and wheat fields. *Biogeosciences*, *10*, 6865–6877. https://doi.org/10.5194/bg-10-6865-2013

Wang, S. R., Di Iorio, D., Cai, W., & Hopkinson, C. S. (2017). Inorganic carbon and oxygen dynamics in a marsh-dominated estuary. *Limnology and Oceanography*, *63*(1), 47–71. https://doi.org/10.1002/lno.10614

Washbourne, I. J., Crenshaw, C. L., & Baker, M. A. (2011). Dissimilatory nitrate reduction pathways in an oligotrophic aquatic ecosystem: Spatial and temporal trends. *Aquatic Microbial Ecology*, *65*, 55–64. https://doi.org/10.3354/ame01538

Weston, N. B., Neubauer, S. C., Velinsky, J. D., & Vile, M. A. (2014). Net ecosystem carbon exchange and the greenhouse gas balance of tidal marshes along an estuarine salinity gradient. *Biogeochemistry*, *120*, 163–189. https://doi.org/10.1007/s10533-014-9989-7

Wigand, C., Brennan, P., Stolt, M., Holt, M., & Ryba, S. (2009). Soil respiration rates in coastal marshes subject to increasing watershed nitrogen loads in southern New England, USA. *Wetlands*, *29*, 952–963. https://doi.org/10.1672/08-147.1

Wigand,C., Davey, E., Johnson, R., Sundberg, K., Morris, J., Kenny, P., et al. (2015). Nutrient Effects on Belowground Organic Matter in a Minerogenic Salt Marsh, North Inlet, SC. *Estuaries and Coasts*, *38*(6), 1838–1853. http://doi.org/10.1007/s12237-014-9937-8

Wigand, C., Sundberg, K., Hanson, A., Davey, E., Johnson, R., Watson, E., & Morris, J. (2016). Varying inundation regimes differentially affect natural and sand-amended marsh sediments. *PLoS ONE*, *11*(10), e0164956. https://doi.org/10.1371/journal.pone.0164956

Wilson, B. J., Mortazavi, B., & Kiene, R. P. (2015). Spatial and temporal variability in carbon dioxide and methane exchange at three coastal marshes along a salinity gradient in a northern Gulf of Mexico estuary. *Biogeochemistry*, *123*(3), 329–347. https://doi.org/10.1007/s10533-015-0085-4

Windham-Myers, L., Wei-Jun, C., Alin, S., Andersson, A., Crosswell, J., Dunton, K., et al. (2018). N. Cavallaro, G. Shrestha, R. Birdsey, M. A. Mayes, R. G. Najjar, S. C. Reed, P. Romero-Lankao & Z. Zhu (Eds.), *Second state of the carbon cycle report: Chapter 15 tidal wetlands and estuaries* (596–648). U.S. Global Change Research Program. https://doi.org/10.7930/SOCCR2.2018.Ch15

Zawatski, M. (2018). *Carbon exchange and sediment deposition in a heterogeneous New England salt marsh (Unpublished master's thesis).* Villanova, PA, USA: Villanova University.